Supplementary Material

Forward signal simulation in impermeable spheres with gamma distributed radii

The ability of the two-parameter model Eq. (18) — repeated below as Eq. (S1) — to adequately describe diffusion in heterogeneous systems in which there exists a distribution of restriction length scales is explored here by forward simulating the signal in impermeable spheres with a known gamma distribution of radii, $P(R)$, and subsequently fitting the simulated ΔI to obtain f_m and $\langle c \rangle$.

$$\Delta I(b_s, t_m = 0) = f_m \left[\exp\left(-b_s^{1/3} \langle c \rangle\right) - \exp\left(-2^{2/3} b_s^{1/3} \langle c \rangle\right) \right]. \tag{S1}$$

From Neuman (1974), the normalized spin echo attenuation due to diffusion within an impermeable sphere of radius R under a static field gradient with amplitude g and echo time 2τ is given by

$$\frac{I}{I_0} = \exp\left(-\frac{2\gamma^2 g^2}{D_0} \sum_{m=1}^{\infty} \frac{\alpha_m^{-4}}{\alpha_m^2 - 1} \left[2\tau - \frac{3 - 4\exp\left(-\alpha_m^2 D_0 \tau\right) + \exp\left(-2\alpha_m^2 D \tau\right)}{\alpha_m^2 D_0} \right] \right), \tag{S2}$$

where γ is the gyromagnetic ratio, D_0 is the free diffusivity, α_m is the mth root of

$$\alpha_m R J'_{3/2}(\alpha_m R) - \tfrac{1}{2} J_{3/2}(\alpha_m R) = 0, \tag{S3}$$

where $J_{3/2}$ is a Bessel function of the first kind and for which the first five roots are $\alpha_m R = [2.0815, 5.940, 9.206, 12.405, 15.579]$. To simulate data, 2000 radii were selected from a gamma distribution, $\gamma(\alpha, \beta)$, with parameters α and β using the `gamrnd` function in MATLAB. Radii (in μm) were then normalized by a factor of $\beta/(3\alpha)$ and constrained to between 0.1 and 3.5. More explicitly,

$$R \sim \min\left\{ \left(\frac{\beta}{3\alpha}\right) \gamma(\alpha, \beta) + 0.1, 3.5 \right\} \ \mu\text{m}. \tag{S4}$$

Larger values of R are ignored because $R = 3.5\ \mu$m is sufficient to fully attenuate the signal at the τ and b-values used. Values of ΔI were then simulated by choosing τ_1 and τ_2 to satisfy the $b_d = b_s$ and $b_d = 0$ conditions discussed in the main text, simulating I/I_0 with the first five roots, and averaging over all spheres. Experimental parameters were kept consistent with the main text: $D_0 = 2.15\ \mu\text{m}^2/\text{ms}$, $g = 15.3\ \text{T/m}$. No noise was added as the purpose of this supplement is merely to demonstrate correspondence between $P(R)$ and fit parameters f_m and $\langle c \rangle$. Results for several α and β are shown in Fig. S1. The PDF of radii $P(R)$, the simulated double and single spin echo signals, and the fitted ΔI are plotted. The truncated region of fit was chosen to be $b_s = [2, 5]\ \text{ms}/\mu\text{m}^2$, as described in the Results section of the main text.

In all cases, the simulated ΔI is adequately fit by Eq. (S1) in the truncated region. Note, however, that the same systematic overestimation at low and high b_s seen in the experimental data (Fig. 6A) is observed here. Changes in f_m and $\langle c \rangle$ correspond to the changes in $P(R)$. As the $P(R)$ distribution shifts to the right in Figs. S1A–C (same α, increasing β), f_m decreases whilst $\langle c \rangle$ increases, indicating a smaller fraction of restricted water and a distribution of radii that is further to the right (closer to ℓ_g), as expected. In Fig. S1D, $P(R)$ is shifted left, decreasing $\langle c \rangle$ compared to Fig. S1A because the central peak of $P(R)$ now lies to the left of ℓ_g. Thus, fitting to Eq. (S1) yields apparent parameters that meaningfully reflect coarse changes in $P(R)$ (sans exchange), at least in cases where the analytical signal models in Neuman (1974) may be applied, i.e., when the Gaussian phase approximation is valid — see Axelrod and Sen (2001).

While the simulation results indicate that estimated parameters from a simplified two-parameter model trend correctly with $P(R)$, the fit quality is noticeably better as $P(R)$ decreases below l_g. Further, we see that the simulation Fig. S1D is the closest to the experimental results, providing an initial indication that the majority of restricted water is restricted on length scales less than 800 nm in the neonatal mouse spinal cord.

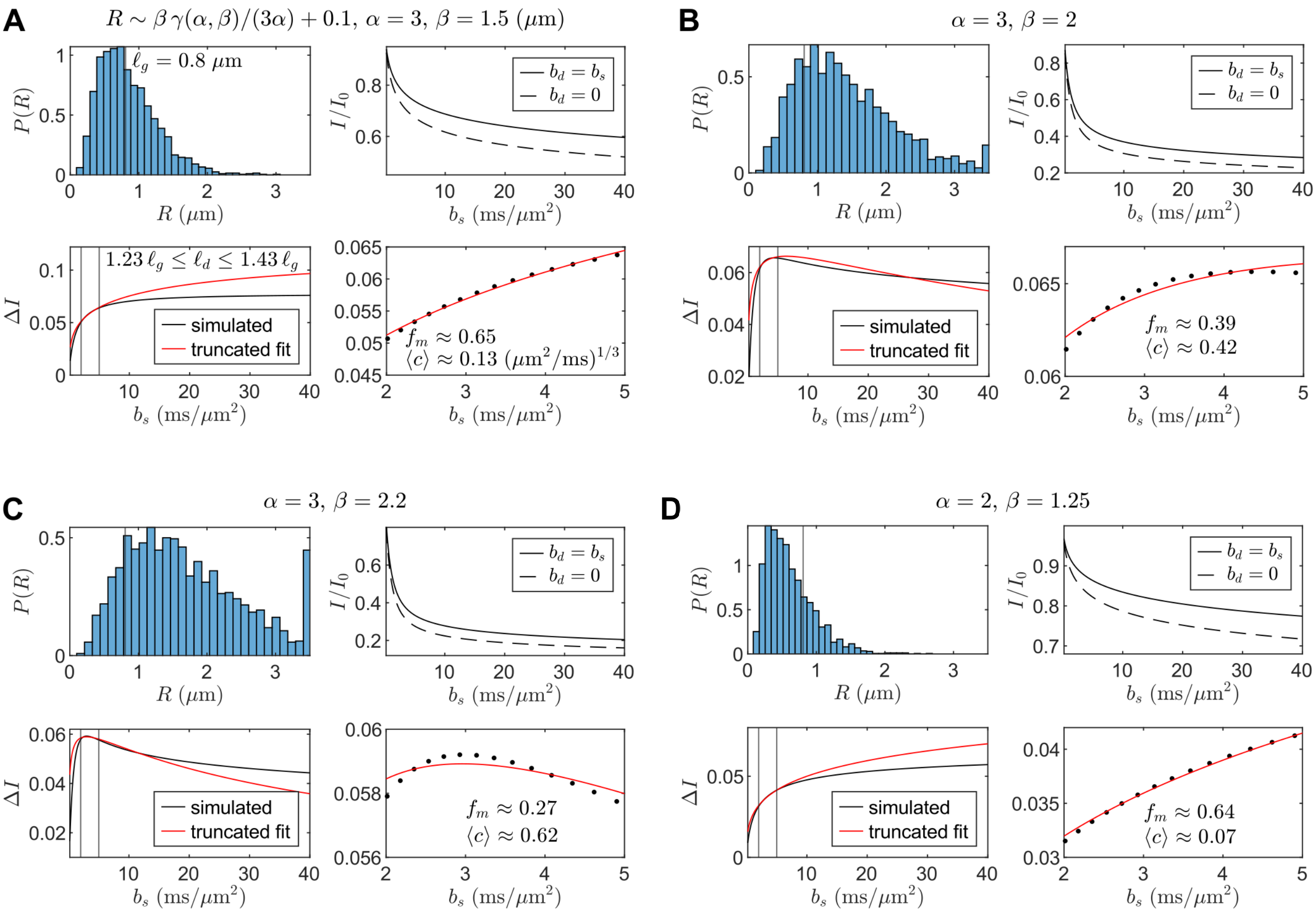

Figure S1. Simulated data and fits from impermeable spheres with gamma distributed radii. (**A**) Histogram of simulated $P(R)$ with $\alpha = 3$ and $\beta = 1.5$. The dephasing length $\ell_g = 0.8\ \mu\mathrm{m}$ is overlaid. Signal was averaged over 2000 spheres to obtain I/I_0 in the single ($b_d = b_s$) and double spin echo ($b_d = 0$) cases, shown to the right. The simulated difference ΔI is then compared to the truncated fit with truncation range $b_s = [2, 5]\ \mathrm{ms}/\mu\mathrm{m}^2$. In all cases, fits were performed using `lsqnonlin` and an initial guess of $f_m = 0.6$ and $\langle c\rangle = 1 \times 10^{-5}\ (\mu\mathrm{m}^2/\mathrm{ms})^{1/3}$ was provided. The truncated region is plotted to the right along with fitted f_m and $\langle c\rangle$ values. Data was simulated in increments of $\tau = 1.5 \times 10^{-2}$ ms. The fit yields estimates $f_m = 0.65$ and $\langle c\rangle = 0.13\ (\mu\mathrm{m}^2/\mathrm{ms})^{1/3}$. (**B**) Simulation with $\alpha = 3$, $\beta = 2$ yields $f_m = 0.39$, $\langle c\rangle = 0.42$. (**C**) Simulation with $\alpha = 3$, $\beta = 2.2$ yields $f_m = 0.27$, $\langle c\rangle = 0.62$. (**D**) Simulation with $\alpha = 2$, $\beta = 1.25$ yields $f_m = 0.64$, $\langle c\rangle = 0.07$. Note that this final case closely resembles the experimental data presented in Fig. 6A

Analysis of different truncation points

In the main text, a theoretical justification for the chosen truncation range of $b_s = [2, 5]$ ms$/\mu$m^2 or $1.23\,\ell_g \leq \ell_d \leq 1.6\,\ell_g$ was given. Of course, a smaller range will yield better fits in general. As such, it is appropriate to empirically explore the effect of different truncation points and thereby provide further justification of the proposed truncation procedure. In Fig. S2, every available point in Fig. 6A is utilized as an alternative truncation point. In each case, $b_s = 2$ ms$/\mu$m^2 remains the minimum point. The obtained fit parameters and residual sum of squares (RSS) over the truncation region are plotted in Fig. S2B. As

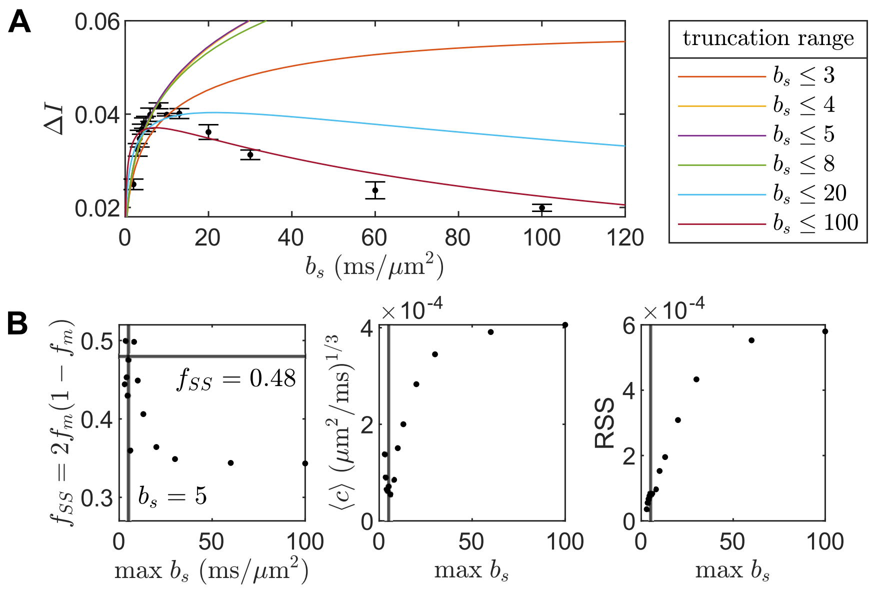

Figure S2. Analysis of alternative b_s truncation points. (**A**) Data from Fig. 6A with fits using $b_s = 2$ms$/\mu$m^2 as the minimum and different b_s values as the maximum of the truncation range. (**B**) Obtained fit parameters and RSS over the truncation region for different maximum b_s. Note that fit parameters and RSS values converge as b_s nears 5 ms$/\mu$m^2. The convergent f_m values agree with the experimentally observed steady-state exchange fraction f_{SS}, i.e., at long mixing time.

expected, the RSS decreases as the range decreases. It is also clear, however, that the obtained fit parameters f_m and $\langle c \rangle$ stabilize as the truncation point nears $b_s = 5$ ms$/\mu$m^2. Furthermore, the calculated steady-state exchanging fraction, $f_{SS} = 2f_m(1 - f_m)$, converges on the experimentally observed value of 0.48 shown in Fig. 6C (with the exception of a single outlier). Similar convergence is also observed for the fitting of k using different b_s as the fixed value (data not shown). Thus, there is good empirical justification for the choice to truncate at or near $b_s = 5$ ms$/\mu$m^2, in addition to the presented theoretical arguments.

REFERENCES

Neuman C. Spin echo of spins diffusing in a bounded medium. *The Journal of Chemical Physics* **60** (1974) 4508–4511.

Axelrod S, Sen PN. Nuclear magnetic resonance spin echoes for restricted diffusion in an inhomogeneous field: Methods and asymptotic regimes. *The Journal of Chemical Physics* **114** (2001) 6878–6895.